PHYSICAL REVIEW D **95,** 083509 (2017)

Magnetogenesis during inflation and preheating in the Starobinsky model

S. Vilchinskii,[1,2] O. Sobol,[1] E. V. Gorbar,[1,3] and I. Rudenok[1]

[1]*Department of Physics, Taras Shevchenko National University of Kyiv, Kyiv 03022, Ukraine*
[2]*Département de Physique Théorique, Center for Astroparticle Physics, Université de Genève, 1211 Genève 4, Switzerland*
[3]*Bogolyubov Institute for Theoretical Physics, Kyiv 03680, Ukraine*

(Received 13 February 2017; published 10 April 2017)

By assuming the kinetic coupling $f^2(\phi)FF$ of the effective inflaton field ϕ with the electromagnetic field, we explore magnetogenesis during the inflation and preheating stages in the R^2 Starobinsky model. We consider the case of the exponential coupling function $f(\phi) = \exp(\alpha\phi/M_p)$ and show that for $\alpha \sim 12$–15 it is possible to generate the large-scale magnetic fields with strength $\gtrsim 10^{-15}$ Gauss at the present epoch. The spectrum of generated magnetic fields is blue with the spectral index $n = 1 + s$, $s > 0$. We have found that for the relevant values of the coupling parameter, $\alpha = 12$–15, the model avoids the backreaction problem for all relevant modes.

DOI: 10.1103/PhysRevD.95.083509

I. INTRODUCTION

A variety of observations imply that stars, galaxies, and clusters of galaxies are all magnetized. The typical magnetic field strengths range from a few μG in the case of galaxies and galaxy clusters up to 10^{15} G in magnetars (see, e.g., Refs. [1–7]. The upper and lower bounds on the strength of the present large-scale magnetic fields B_0 are given as 10^{-17} G $\lesssim B_0 \lesssim 10^{-9}$ G by the observations of the cosmic microwave background (CMB) [8,9] and the gamma rays from blazars [10–13], respectively. The origin and evolution of these magnetic fields are the subject of intense studies.

Two classes of models for the origin of these magnetic fields are generally discussed (for a review, see Refs. [4–7]). One possibility is that the observed fields result from the amplification during the structure formation of primordial magnetic fields produced in the early Universe. Another logical possibility is that the observed magnetic fields are of a purely astrophysical origin. The recent multifrequency blazar observation of large-scale magnetic fields in voids [10–13] with strength not less than 10^{-16} G [11] coherent on a Mpc scale supports the case for primordial magnetic fields.

Various cosmological phase transitions could be considered as one of the possible ways of producing primordial magnetic fields [14–19]. However, the comoving coherence length of such magnetic fields cannot be larger than the Hubble horizon at the phase transition, which is much smaller than Mpc today. Consequently, the most natural mechanism for the generation of the large-coherence-scale magnetic fields is inflation in the early Universe [20] through the exponential stretching of wave modes during the accelerated expansion.

It is well known that quantum fluctuations of massless scalar and tensor fields are very strongly amplified in the inflationary stage and create considerable density inhomogeneities evolving later into the large-scale structure of the observed Universe [21–25] or relic gravitational waves [26–28]. However, since the Maxwell action is conformally invariant, the fluctuations in the electromagnetic field are not enhanced in the conformally flat expanding background of inflation [29]. Therefore, in order to generate magnetic fields, one needs to break conformal invariance of the electromagnetic field, e.g., by coupling it to a scalar or a pseudoscalar field or to a curvature invariant. Although many ways to break the conformal invariance of the electromagnetic action during inflation were suggested in the literature [30–34], we adopt in our study the kinetic coupling model f^2FF firstly introduced by Ratra [30], where f is a function of the inflaton field ϕ and F is the electromagnetic field tensor. Depending on the form of the coupling f, this gives rise to different magnetic field power spectra [30,35–40]. Alternative models, in which magnetogenesis is driven by a rolling pseudo Goldstone boson φ through its coupling to the electromagnetic field in the form $\varphi F\tilde{F}$, are also very interesting and much studied [41–47].

According to the most recent observational data by the Planck Collaboration [48], the R^2 model proposed by Starobinsky in 1980 [49] is the most favored among the models of inflation. For example, the chaotic inflationary models like large field inflation and natural inflation are disfavored due to their high tensor-to-scalar ratio. Therefore, we will study the inflationary magnetogenesis in the Starobinsky model in the present paper, which to the best of our knowledge was not previously investigated in the literature. It is worth mentioning also that supergravity motivates a potential similar to the Einstein gravity conformal representation of the R^2 inflationary model [50–54].

If the conformal invariance of the electromagnetic action is broken, the generation of cosmological magnetic fields can occur after inflation before reheating, where the conductivity of the Universe becomes high, during the preheating stage [55]. In this epoch, the inflaton field oscillates around its potential minimum and the Universe is effectively dominated by cold matter. Depending on the coupling between the inflaton and matter fields, this process sometimes could proceed nonperturbatively and parametric resonance may play a crucial role for bosonic fields [56,57]. Since the electromagnetic field could be significantly amplified during preheating [55,58–64], we study also the postinflationary amplification of magnetic fields in the present paper and quantify how it affects the magnetic fields generated during inflation and preheating in the Starobinsky model.

This paper is organized as follows. We solve the background equations of the Starobinsky model during inflation and preheating in Sec. II. In Sec. III, we consider the kinetic coupling of the inflaton field ϕ to the electromagnetic field, calculate the energy density of the generated magnetic fields and then determine and analyze the evolution of the magnetic energy density through the subsequent stages of inflation and preheating. The summary of the obtained results is given in Sec. IV.

II. INFLATON EVOLUTION DURING INFLATION AND PREHEATING

Historically, one of the first models that exhibited inflation was the model suggested by Starobinsky [49], whose gravitational action reads as

$$S_{gr} = -\frac{M_p^2}{2}\int d^4x\sqrt{-g}\left[R - \frac{R^2}{6\mu^2}\right], \tag{1}$$

where $g = \det g_{\lambda\nu}$, in which $g_{\lambda\nu}$ is a metric tensor; $\mu = 1.3\times 10^{-5}M_p$ is a constant, which is fixed by the requirement to have the correct magnitude of the primordial perturbations [65]; and $M_p = \frac{M_{\rm Pl}}{\sqrt{8\pi}} = 2.4\times 10^{18}$ GeV is the reduced Planck mass. A conformal transformation $g_{\lambda\nu}\to\chi^{-1}g_{\lambda\nu}$ with $\chi = \exp\left(\sqrt{\frac{2}{3}}\frac{\phi}{M_p}\right)$ transforms the Lagrangian of theory (1) into that of the usual Einstein gravity with a new spatially uniform scalar field ϕ (inflaton), whose potential reads

$$V(\phi) = \frac{3\mu^2}{4}\left(1 - \exp\left[-\sqrt{\frac{2}{3}}\phi\right]\right)^2. \tag{2}$$

It is quadratic in the vicinity of its minimum at $\phi = 0$ and becomes flat at large values of ϕ.

The time evolution of the Friedmann-Lemaıtre-Robertson-Walker (FLRW) universe with zero spatial curvature is described by the Friedmann equation

$$H^2 = \frac{1}{3M_p^2}\left(\frac{1}{2}\dot{\phi}^2 + V(\phi)\right), \tag{3}$$

and the equation of motion for the inflaton field in the FLRW universe reads

$$\ddot{\phi} + 3H\dot{\phi} + \frac{\partial V}{\partial\phi} = 0, \tag{4}$$

where $H\equiv\frac{\dot{a}}{a}$ is the Hubble parameter and $a = a(t)$ is the scale factor. It is convenient to use the dimensionless quantities, where the inflaton field and Hubble parameter are expressed in Planck masses M_p, time in M_p^{-1}, and the Lagrangian density and inflaton effective potential in M_p^4.

The Universe expands quasiexponentially during the inflation stage. In this regime the potential term dominates the kinetic one in Eq. (3) and the "friction" term $3H\dot{\phi}$ dominates $\ddot{\phi}$ in Eq. (4). The slow-roll parameters for inflaton potential (2) equal

$$\epsilon = \frac{1}{2}\left(\frac{V'}{V}\right)^2 = \frac{4}{3(\exp[\sqrt{\frac{2}{3}}\phi] - 1)^2},$$

$$\eta = \frac{V''}{V} = \frac{4(2-\exp[\sqrt{\frac{2}{3}}\phi])}{3(\exp[\sqrt{\frac{2}{3}}\phi] - 1)^2} \tag{5}$$

(here prime denotes derivatives with respect to the inflaton). Inflation lasts until the slow-roll conditions are satisfied $\epsilon\ll 1$, $|\eta|\ll 1$. The duration of the inflation stage $t_{\rm inf}\simeq\frac{3}{2\mu}e^{\sqrt{\frac{2}{3}}\phi_i}$ depends on the initial value of the inflaton ϕ_i. The minimal number of e-folds $N_e = \ln\frac{a_{\rm inf}}{a_i}\simeq\frac{3}{4}e^{\sqrt{\frac{2}{3}}\phi_i}$ necessary to solve the problems of horizon and flatness of the Universe is approximately $N_{\rm min}\sim 60$–70. This implies $\phi_i = 5.5$ and Eq. (4) in the slow-roll approximation gives the initial value of the time derivative $\dot{\phi}_i = -\frac{V'(\phi_i)}{\sqrt{3V(\phi_i)}}$.

To determine the time dependence of the inflaton field and the scale factor, Eqs. (3) and (4) were integrated with the initial conditions, discussed above, and the following approximate solution has been obtained by using the slow-roll conditions:

$$a(t) = \exp\left(\frac{\mu t}{2}\right)\left[1 - \frac{t}{t_{\rm inf}}\right]^{3/4}, \tag{6}$$

$$\phi(t) = \phi_i + \sqrt{\frac{3}{2}}\ln\left[1 - \frac{t}{t_{\rm inf}}\right]. \tag{7}$$

This solution satisfactorily fits the numerical solution to Eqs. (3) and (4) for $\mu(t_{\rm inf} - t)\gg 1$. The time dependence of the inflaton is plotted in the left panel in Fig. 1. The time dependences of the scale factor and the slow-roll parameters are plotted in Fig. 2.

The inflaton field during preheating after the end of inflation behaves like a dust (pressure $p = 0$); therefore,

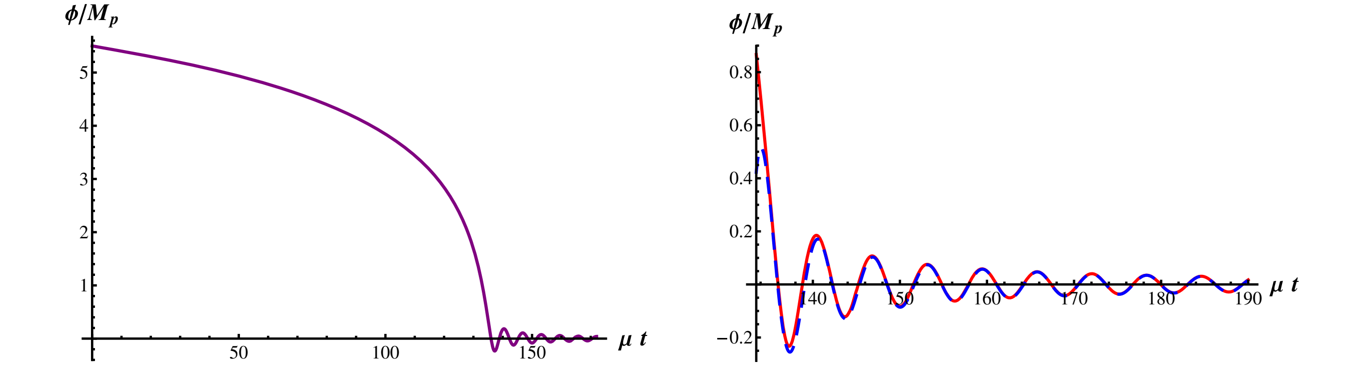

FIG. 1. Left panel: The time dependence of the inflaton field during and after inflation. Right panel: Oscillations of the inflaton field after the end of inflation (red solid line) and the approximate function (blue dashed line).

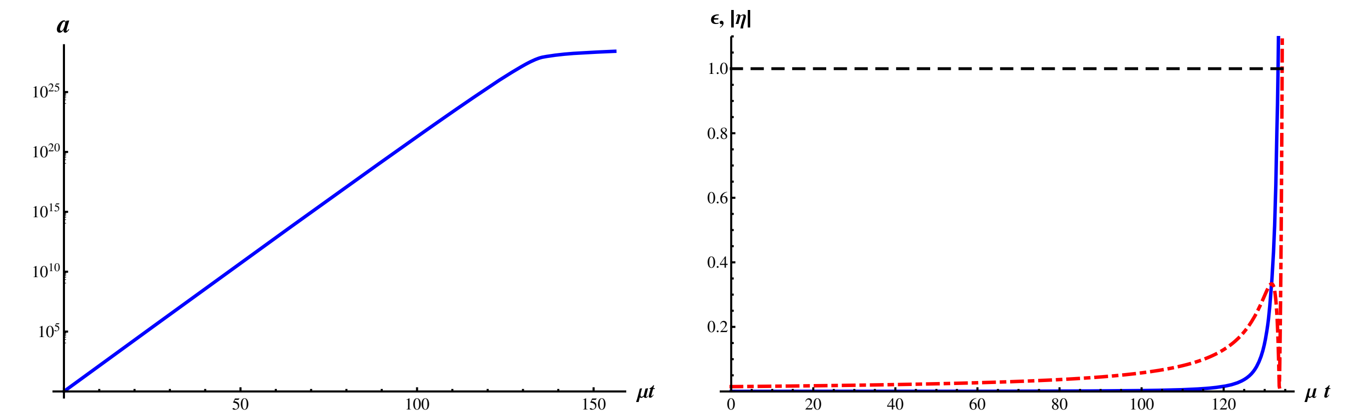

FIG. 2. Left panel: The time dependence of the scale factor during inflation and preheating. Right panel: The time dependence of the slow-roll parameters ϵ (blue solid line) and η (red dashed-dotted line) during inflation.

$a \sim (t - t_s)^{2/3}$, where t_s is the moment of time when the Universe became dust dominated. Since the amplitude of fast oscillations decreases in time as $\sim a^{-3/2}$, the approximate solution during the preheating stage is $\phi(t) = \frac{C}{\mu(t-t_s)} \sin[\mu(t - t_0)]$, where $C = \sqrt{8/3}$ was found by taking into account that the inflaton potential (2) in the vicinity of its minimum behaves like a parabola $V(\phi) \approx \frac{\mu^2\phi^2}{2}$ and the Hubble parameter equals $H = \frac{2}{3(t-t_s)}$ during preheating. The phase shift time t_0 and t_s could be determined numerically from the best fit condition. We found $t_s = 1.008 \times 10^7$ and $t_0 = 1.0216 \times 10^7$. Introducing the shifted time $\tau = t - t_s$, we obtain

$$a(\tau) = a_{\rm inf}\left(\frac{\tau}{\tau_0}\right)^{2/3}, \qquad H(\tau) = \frac{2}{3\tau}, \tag{8}$$

$$\phi(\tau) = \frac{\sqrt{8/3}}{\mu\tau} \sin[\mu(\tau - \tau_0)], \tag{9}$$

where $\mu\tau_0 = 1.77$ and $a_{\rm inf}$ is the value of the scale factor at the end of inflation. The approximate solution (9) is shown in the right panel of Fig. 1 by the blue dashed line. Obviously, it fits the exact solution (red solid line) very well.

III. MAGNETIC FIELD GENERATION

In order to study magnetogenesis in the Starobinsky model, we consider the kinetic coupling of the inflaton field ϕ to the electromagnetic field $F_{\lambda\nu} \equiv \partial_\lambda A_\nu - \partial_\nu A_\lambda$, characterized by its four-vector potential A_ν,

$$S_{\rm int} = \int d^4x \sqrt{-g}\mathcal{L}_{\rm int}, \qquad \mathcal{L}_{\rm int} = -\frac{f^2(\phi)}{4} F_{\lambda\nu}F^{\lambda\nu}, \tag{10}$$

where $F^{\lambda\nu} = g^{\lambda\gamma}g^{\beta\nu}F_{\gamma\beta}$, and $f(\phi)$ is the coupling function introduced by Ratra [30]

$$f(\phi) = \exp(\alpha\phi). \tag{11}$$

This function with free parameter α gives the correct value $f = 1$ after the end of preheating and, consequently, the correct value of the electron charge today. In addition, this function does not cause the strong coupling problem during the inflation stage, where $\phi \gg 1$.

The equation of motion for the electromagnetic vector potential in the Coulomb gauge $A_0 = 0$, $\partial_i A^i = 0$ has the form

$$\ddot{A}_i(t,x) + \left(H + 2\frac{\dot{f}}{f}\right)\dot{A}_i(t,x) - \partial_j\partial^j A_i(t,x) = 0. \tag{12}$$

Quantizing the electromagnetic field, the vector potential can be decomposed into the sum over creation $\hat{b}^\dagger_{k,\lambda}$ and annihilation operators $\hat{b}_{k,\lambda}$:

$$\hat{A}_j(t,x) = \int \frac{d^3k}{(2\pi)^{2/3}} \times \sum_{\lambda=1}^{2}[\epsilon_j^\lambda(k)\hat{b}_{k,\lambda}A(t,k)e^{ik\cdot x} + \epsilon_j^{*\lambda}(k)\hat{b}^\dagger_{k,\lambda}A^*(t,k)e^{-ik\cdot x}], \tag{13}$$

where $\epsilon_j^\lambda(k)$, $\lambda = 1,\ 2$, are two independent transverse polarization vectors. The time evolution of the function $\mathcal{A}(t,k) = f(t)a(t)A(t,k)$ is governed by the equation

$$\ddot{\mathcal{A}}(t,k) + H\dot{\mathcal{A}}(t,k) + \left(\frac{k^2}{a^2(t)} - H\frac{\dot{f}}{f} - \frac{\ddot{f}}{f}\right)\mathcal{A}(t,k) = 0. \tag{14}$$

The scale factor $a(t)$ in the definition of $\mathcal{A}$ originates from the presence of the polarization vectors ϵ_j^λ in the Fourier expansion (13), which contain the scale factor in their explicit expressions [37].

One rewrites this equation in conformal time $\eta(t) = \int^t \frac{dt'}{a(t')}$ as

$$\mathcal{A}''(\eta,k) + \left[k^2 - \frac{f''}{f}\right]\mathcal{A}(\eta,k) = 0, \tag{15}$$

where prime denotes derivatives with respect to the conformal time. We can determine the initial condition to Eq. (15) from the asymptotic behavior in the early stages, where we assume $f = f(\phi_i) = \text{const}$, that gives

$$\mathcal{A} \simeq \mathcal{A}_{\text{free}}(\eta,k) = \frac{1}{\sqrt{2k}}e^{-ik\eta}, \qquad -k\eta \gg 1. \tag{16}$$

Covariantly defined electric and magnetic fields seen by an observer characterized by the 4-velocity vector u^μ have the following form [66]:

$$E_\mu = u^\nu F_{\mu\nu}, \qquad B_\mu = \frac{1}{2}\eta_{\mu\nu\rho\sigma}F^{\nu\rho}u^\sigma, \tag{17}$$

where $\eta_{\mu\nu\rho\sigma}$ is the totally antisymmetric tensor with $\eta_{0123} = \sqrt{-g}$. For the comoving observer with $u^\mu = (1,\vec{0})$, we find in the Coulomb gauge

$$E_i = -\partial_t A_i, \qquad B_i = \frac{1}{a}\epsilon_{ijk}\partial_j A_k, \tag{18}$$

with $\epsilon_{123} = 1$.

The interaction Lagrangian (10) makes the following contribution to the stress-energy tensor:

$$T_{\lambda\nu} = -\frac{2}{\sqrt{-g}}\frac{\delta S_{\text{int}}}{\delta g^{\lambda\nu}} = -f^2(\phi)g^{\gamma\beta}F_{\lambda\gamma}F_{\beta\nu} + g_{\lambda\nu}\mathcal{L}_{\text{int}}. \tag{19}$$

Then, we could determine the energy density of the electromagnetic field as $\rho = -\langle T_0^0\rangle$. The "magnetic" part of the energy density ρ_B does not contain time derivatives of the vector potential $\partial_0 A_i$, while only the "electric" part ρ_E contains such derivatives. They equal [37]

$$\rho_B(t) = \int_0^{+\infty}\frac{dk}{k}\frac{d\rho_B(t,k)}{d\ln k} = \frac{1}{2\pi^2}\int_0^{+\infty}\frac{dk}{k}\left(\frac{k}{a(t)}\right)^4 k|\mathcal{A}(t,k)|^2, \tag{20}$$

$$\rho_E(t) = \int_0^{+\infty}\frac{dk}{k}\frac{d\rho_E(t,k)}{d\ln k} = \frac{1}{2\pi^2}\int_0^{+\infty}\frac{dk}{k}\left(\frac{k}{a(t)}\right)^2 kf^2(t)\left|\frac{\partial}{\partial t}\left(\frac{\mathcal{A}(t,k)}{f(t)}\right)\right|^2. \tag{21}$$

Numerically solving Eq. (14) with the corresponding boundary conditions, we determine the vector potential $\mathcal{A}(t,k)$ and the power spectrum of generated magnetic and electric fields $\frac{d\rho_B(t,k)}{d\ln k}$ and $\frac{d\rho_E(t,k)}{d\ln k}$.

Once we obtained the spectrum of the magnetic field, we should rescale it up to the present time. For this, we should determine the value of the scale factor at the present time compared to its value at the end of preheating:

$$\frac{a_0}{a_e} \sim \frac{T_{\max}}{T_0}. \tag{22}$$

If we take $T_{\max} \sim 10^{15}$ GeV and $T_0 = 2.3 \times 10^{-13}$ GeV, we obtain

$$\frac{a_0}{a_e} \sim 10^{28}. \tag{23}$$

The authors of Ref. [5] defined the so-called cosmic diffusion length as the minimal size of a magnetic configuration which can survive diffusion during the Universe's lifetime and estimated it as $r_{\text{diff}} \sim 1$ A.U. $= 1.5 \times 10^{13}$ cm. The corresponding wave vector in our epoch is $k_{\text{diff}}/a_0 \sim 1$ A.U.$^{-1} \approx 1.3 \times 10^{-27}$ GeV. Therefore, in what follows, we will be interested only in modes with $k < k_{\text{diff}}$.

A. Magnetogenesis during inflation

It is interesting to follow the time evolution of the amplitude of a given mode. The left panel in Fig. 3

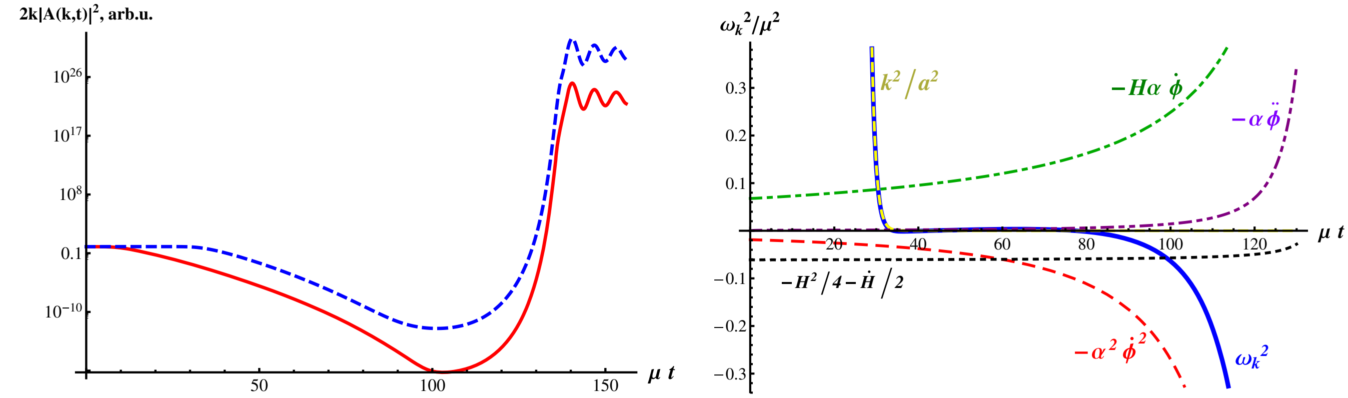

FIG. 3. Left panel: The time dependence of the square modulus of the electromagnetic potential $2k|\mathcal{A}(k,t)|^2$ for two different modes $k = 10\mu$ (red solid line) and $k = 10^6\mu$ (blue dashed line) for $\alpha = 15$. Right panel: The function $\omega_k^2(t)$ (blue solid line) defined by Eq. (25) and its constituent terms $\frac{k^2}{a^2(t)}$ (yellow dashed line), $-H\alpha\dot{\phi}$ (green dashed-dotted line), $-\alpha^2\dot{\phi}^2$ (red dashed line), $-\alpha\ddot{\phi}$ (purple dashed-dotted line with two dots), and $-\frac{1}{4}H^2 - \frac{1}{2}\dot{H}$ (black dotted line). The function and the corresponding terms are plotted for $\alpha = 15$ and $k = 10^6\mu$.

shows the time dependence of the square modulus of the electromagnetic potential $2k|\mathcal{A}(k,t)|^2$ for two different momenta. When the mode is inside the horizon ($k > aH$) it oscillates in time without significant changes of its amplitude (see the blue dashed line in the left panel of Fig. 3 for $\mu t \lesssim 30$). As the mode crosses the horizon its amplitude decreases due to the Universe's expansion (see Fig. 3 for $30 \lesssim \mu t \lesssim 100$). Therefore, the earlier the mode crosses the horizon, the smaller the amplitude it has at the end (compare the red and blue curves in Fig. 3). This process lasts nearly to the end of inflation, when the evolution of the inflaton field starts to deviate from the slow-rolling regime. Let us rewrite Eq. (14) in terms of a rescaled field $\mathcal{F}(t,k) = a^{1/2}(t)\mathcal{A}(t,k)$:

$$\ddot{\mathcal{F}}(k,t) + \omega_k^2(t)\mathcal{F}(k,\tau) = 0,$$
$$\omega_k^2(t) = \frac{k^2}{a^2(t)} - H\frac{\dot{f}}{f} - \frac{\ddot{f}}{f} + \frac{1}{4}H^2 - \frac{1}{2}\frac{\ddot{a}}{a}. \qquad (24)$$

Taking into account the explicit form of the coupling function (11), we can represent ω_k^2 as follows:

$$\omega_k^2(t) = \frac{k^2}{a^2(t)} - H\alpha\dot{\phi} - \alpha^2\dot{\phi}^2 - \alpha\ddot{\phi} - \frac{1}{4}H^2 - \frac{1}{2}\dot{H}. \qquad (25)$$

Let us examine the behavior of different terms in Eq. (25) using expressions (6) and (7):

$$-H\alpha\dot{\phi} \simeq \frac{\sqrt{6}}{4}\frac{\mu^2\alpha}{(\mu t_{\rm inf} - \mu t)} > 0,$$
$$-\alpha^2\dot{\phi}^2 \simeq -\frac{3}{2}\frac{\mu^2\alpha^2}{(\mu t_{\rm inf} - \mu t)^2} < 0,$$
$$-\alpha\ddot{\phi} \simeq \frac{\sqrt{6}}{2}\frac{\mu^2\alpha}{(\mu t_{\rm inf} - \mu t)^2} > 0,$$
$$H^2 \lesssim \frac{\mu^2}{4},$$
$$\dot{H} \simeq -\frac{3}{4}\frac{\mu^2}{(\mu t_{\rm inf} - \mu t)^2}.$$

To estimate each of these terms we must take into account that $\mu t_{\rm inf} = 3/2\exp(\sqrt{2/3}\phi_i) \approx 130 \gg 1$ for our choice of the inflaton initial value $\phi_i = 5.5$. At the beginning of the inflation when $t \ll t_{\rm inf}$, the largest values have k^2/a^2, H^2, and the term with the first power of $(\mu t_{\rm inf} - \mu t)$ in the denominator, namely, $-H\alpha\dot{\phi} > 0$. However, near the end of inflation the other terms could not be neglected. Their relative contributions depend on the coefficients in the numerators. Since we consider $\alpha \sim 10$–$20 \gg 1$, the term $-\alpha^2\dot{\phi}^2 < 0$ dominates the rest of the terms in Eq. (25). The moment of time when this happens could be estimated as $\mu(t_{\rm inf} - t) \sim \sqrt{6}\alpha$ when the second and third terms in Eq. (25) are equal by the absolute values. This condition could also be expressed in terms of the slow-roll parameters. The third term on the right-hand side of Eq. (25) starts to dominate, when $\alpha\dot{\phi}/H \sim \sqrt{2\epsilon}\alpha/3 \gtrsim 1$. For $\alpha \sim 10$–20, this happens for $\sqrt{\epsilon} \sim \eta \sim 0.1$ (see the right panel in Fig. 2).

We illustrate this behavior of the function $\omega_k^2(t)$ in the right panel of Fig. 3. As the figure shows, the function $\omega_k^2(t)$ turns its sign to negative at $\mu t \simeq 90$ and an instability occurs. It is important that for all modes, which have

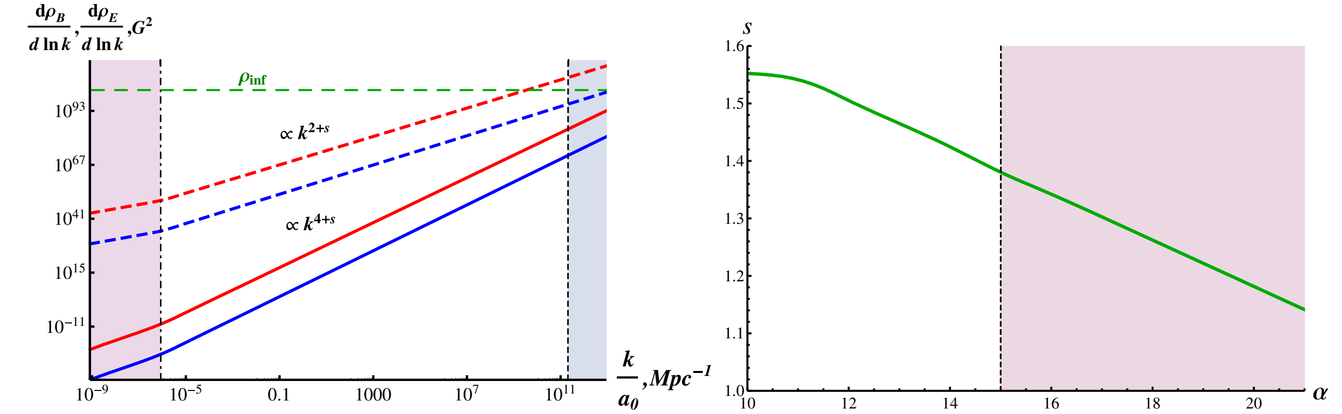

FIG. 4. Left panel: The power spectrum of magnetic (solid lines) and electric (dashed lines) fields generated during inflation for $\alpha = 12$ (blue lines) and $\alpha = 15$ (red lines). The purple shaded region to the left of the vertical dashed-dotted line separates the nonphysical modes which were outside the horizon even at the beginning of the inflation. The blue shaded region to the right from the vertical dashed line shows the modes with $k/a_0 \gtrsim 1$ A.U. which would not survive diffusion during the evolution of the Universe. The horizontal dashed line shows the energy density of the inflaton field ρ_{inf} during the inflation. Right panel: The dependence of the anomalous slope s on the parameter α. The shaded area is excluded because of the strong backreaction.

already crossed the horizon at that time ($k < aH$), the term k^2/a^2 is suppressed compared to the other terms, especially to $-\alpha^2\dot{\phi}^2$, which causes the instability. As a result, the amplification occurs for all such modes (see the left panel in Fig. 3 for $\mu t > 100$). We would like to emphasize that such an amplification is a built-in property of the model under consideration. Indeed, first, the growth by modulus of the time derivative of the inflaton field near the end of inflation is connected with the form of the effective potential (2) in the Starobinsky model. Second, the presence of the term $-\alpha^2\dot{\phi}^2$ in Eq. (25) is due to the exponential form of the kinetic coupling function. Finally, large values $\alpha \gg 1$ ensure the dominance of this term.

We plot the power spectrum of magnetic and electric fields at the end of inflation in the left panel of Fig. 4 for two different values of parameter α. Clearly, these spectra have similar behavior. Modes that are outside the horizon even at the beginning of the inflation ($k \ll \mu/2$, i.e., $k/a_0 \ll 4\times 10^{-6}$ Mpc^{-1}) are unphysical ones and should not be taken into account. The corresponding region is shaded in purple in the right panel of Fig. 4. For modes that cross the horizon during inflation, the spectrum scales like $\propto k^{4+s}$, where s is the anomalous slope. This behavior is expected to be true up to momenta $k \sim a_{\text{inf}} H_{\text{inf}}$, which cross the horizon at the end of inflation. For larger momenta, the corresponding modes never cross the horizon. Therefore, these modes oscillate in time during the whole inflation stage and undergo neither diminishing nor amplification. As a result, their spectrum remains unchanged and behaves like $\propto k^4$. We are interested among all modes only in those with momenta up to $k/a_0 \sim 1$ A.U. (dashed vertical line), because shorter waves would not survive the cosmic diffusion [5]. Therefore, the spectrum for larger momenta is shaded in blue in Fig. 4.

The power spectrum of the electric fields, generated during inflation, shows much larger values and scales $\propto k^{2+s}$ for modes, which cross the horizon during inflation. It should be noted that the anomalous slope s is the same as that for the magnetic field power spectrum. This numerical fact could be explained as follows. As it could be seen from Eq. (21), the electric field power spectrum is proportional to $f^2|\frac{\partial}{\partial t}(\mathcal{A}/f)|^2 = |\mathcal{A}|^2|\dot{\mathcal{A}}/\mathcal{A} - \alpha\dot{\phi}|^2$. Figure 3 shows that at the end of inflation the mode $\mathcal{A}(k,t)$ does not have the oscillatory behavior $\sim \exp(-ik\eta)$ as at the beginning, but it grows exponentially. The origin of this growth is connected with the fast change of the coupling function at the end of inflation. The rate of this growth does not depend on the momentum for modes with $k \ll a_{\text{inf}} H_{\text{inf}}$, because the term $(k/a)^2$ in Eq. (25) is strongly suppressed at the end of inflation and the term $-\alpha^2\dot{\phi}^2$ dominates. Therefore, the quantity $|\dot{\mathcal{A}}/\mathcal{A} - \alpha\dot{\phi}|^2$ does not depend on k for $k \ll a_{\text{inf}} H_{\text{inf}}$ and it could not change the slope of the spectrum. Then, comparing Eqs. (20) and (21), we conclude that the magnetic and electric power spectra are proportional to $k^5|\mathcal{A}(k,t)|^2$ and $k^3|\mathcal{A}(k,t)|^2$, respectively. As a result, the slopes of these power spectra differ by 2 and they have the same anomalous slope s. The right panel in Fig. 4 shows that the dependence of the anomalous slope s on α is linear and can be approximated as

$$s(\alpha) \approx 1.98 - 0.04\alpha. \tag{26}$$

Let us estimate whether the backreaction problem occurs. According to Refs. [37,67], the model is free of this difficulty when the following condition is satisfied for all modes with $k < k_{\text{diff}}$:

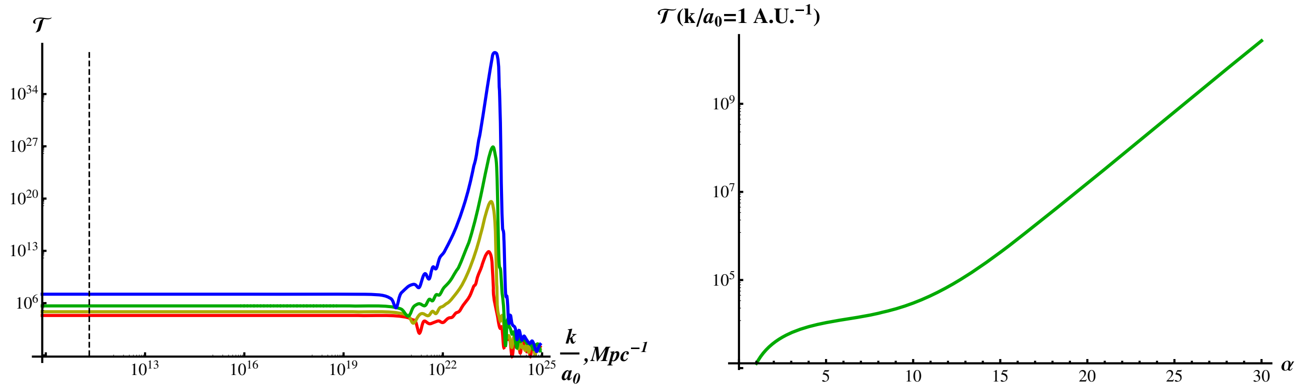

FIG. 5. Left panel: The transfer function of the power spectrum at the end of the preheating stage for $\alpha = 9$ (red line), $\alpha = 12$ (yellow line), $\alpha = 15$ (green line), and $\alpha = 20$ (blue line). The vertical dashed line shows the last mode which survives the cosmic diffusion until the present time. Right panel: The transfer function for the mode with momentum $k/a_0 = 1$ A.U.$^{-1}$ as a function of the parameter α.

$$\left.\frac{d\rho_E(t,k)}{d\ln k}\right|_{\rm inf} + \left.\frac{d\rho_B(t,k)}{d\ln k}\right|_{\rm inf} < \rho_{\rm inf}, \tag{27}$$

where $\rho_{\rm inf}$ is the energy density of the inflaton field during inflation. In our case it could be estimated as

$$\rho_{\rm inf} = 3H_{\rm inf}^2 M_p^2 \approx \frac{3}{4}\mu^2 M_p^2 \sim 10^{103}\ \text{Gauss}^2. \tag{28}$$

It is shown in the left panel of Fig. 4 by a horizontal green dashed line. This figure implies that the backreaction problem does not occur for all cosmologically relevant modes for $\alpha = 12$. As for $\alpha = 15$, condition (27) is violated only near $k_{\rm diff}$. All calculations were done assuming that $a_0/a_e \sim 10^{28}$, which corresponds to $T_{\rm max} \sim 10^{15}$ GeV. The electric part gives the leading contribution to the backreaction and it scales like $\propto (a_0/a_e)^{2+s}$. Therefore, if the maximal temperature during preheating were lower, then the ratio a_0/a_e would be less and the comoving wave number, which corresponds to the present cosmic diffusion scale of 1 A.U., $k_{\rm diff}$, would be lower. As a result, the backreaction problem would be ameliorated.

As it was discussed in Ref. [37], during reheating, the conductivity jumps and, as a consequence, the electric field vanishes. Thus, if one checks that, at the end of inflation, the electric field cannot cause a backreaction problem, then we are guaranteed that the complete scenario is consistent. As we will see in the next subsection, the stage of preheating also contributes to the generated spectrum, but for $\alpha = 12$–15 this contribution is negligible compared to that during inflation; therefore, it cannot cause the backreaction problem, if it was not caused during inflation.

B. Magnetogenesis during preheating

In the previous subsection, we found the power spectrum of the magnetic field generated during the inflation stage. After inflation the scalar field oscillates in the vicinity of the minimum of its potential, producing various particles. It is important to study how these fast oscillations affect the power spectrum of the magnetic fields obtained earlier. For this purpose we define the transfer function $\mathcal{T}(k;\tau,\tau_0)$, which shows the relative enhancement of a given mode k at the moment of time τ compared to the moment of the beginning of the preheating stage τ_0,

$$\mathcal{T}(k;\tau,\tau_0) = \frac{|\mathcal{A}(k,\tau)|^2}{|\mathcal{A}(k,\tau_0)|^2}. \tag{29}$$

Then we obtain the power spectrum at the end of the preheating stage and rescale it to the present time:

$$\left.\frac{d\rho_B}{d\ln k}\right|_{\rm now} = \left.\frac{d\rho_B}{d\ln k}\right|_{\rm inf} \cdot \mathcal{T}(k;\tau_e,\tau_0)\frac{a_e^4}{a_0^4}, \tag{30}$$

where τ_e is the time of the end of the preheating stage, when the amplitude stops increasing.

To obtain the transfer function we have to solve Eq. (14). For the rescaled field $\mathcal{F}(k,\tau) = a^{1/2}(\tau)\mathcal{A}(k,\tau)$ [here τ is a shifted time, defined before Eq. (8)], we obtain Eq. (24), which, taking into account the coupling function (11), Eq. (9), and retaining the monotonous term and the largest oscillating terms in the brackets, could be brought to the Mathieu-like equation by the change of variable $\mu(\tau-\tau_0) = 2z - \pi/2$:

$$\mathcal{F}''(z) + [a_M(k,z) - 2q_M(z)\cos(2z)]\mathcal{F}(z) = 0, \tag{31}$$

where $a_M(k,z) = \frac{4k^2}{\mu^2 a^2(z)} + \frac{8}{9(2z-\pi/2+\mu\tau_0)^2}$ and $q_M(z) = \frac{4\alpha\sqrt{2}}{\sqrt{3}(2z-\pi/2+\mu\tau_0)}$ are the monotonously decreasing functions of z. For constant and sufficiently large q_M the Mathieu equation has exponentially growing solutions. This is the parametric resonance situation. However, $q_M(z)$ decreases with time, the system exits the resonance band, and, as a

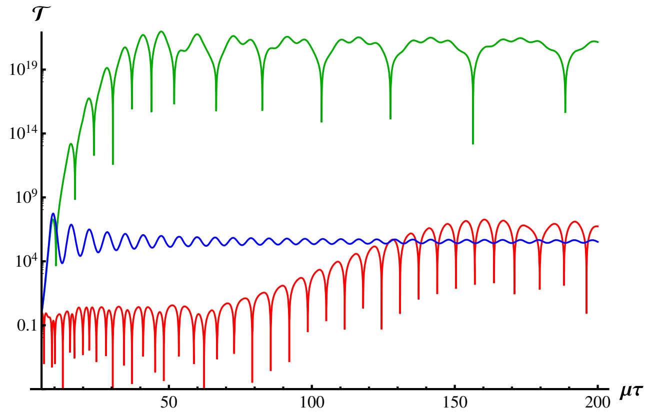

FIG. 6. The time dependence of the transfer function during the preheating stage for three modes $k/a_0 = 2\times 10^{11}$ Mpc^{-1} (blue line), $k/a_0 = 1.5\times 10^{23}$ Mpc^{-1} (green line), and $k/a_0 = 7\times 10^{23}$ Mpc^{-1} (red line).

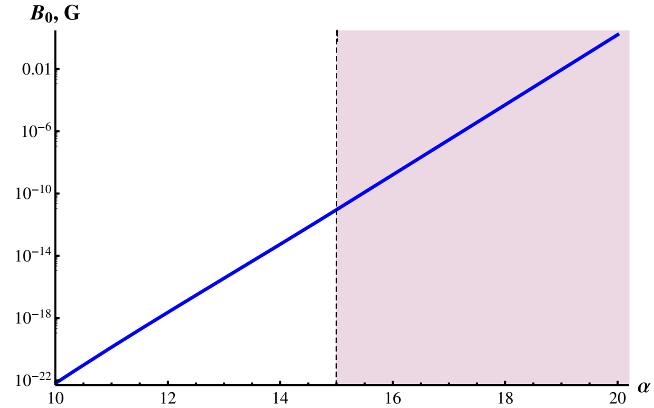

FIG. 7. The generated magnetic field as a function of α. The dashed area is excluded because of the strong backreaction.

result, the exponential growth stops. Therefore, the most considerable enhancement takes place during the first few oscillations of the inflaton.

The transfer function of the power spectrum fixed at $\mu\tau_e = 1000$ (at the end of the preheating stage) is plotted in the left panel of Fig. 5. Obviously, for $k \ll a_{\rm inf}H_{\rm inf}$, i.e., $k/a_0 \ll 10^{21}$ Mpc^{-1}, the transfer function is constant. For modes that reentered the horizon $k \gtrsim a_{\rm inf}H_{\rm inf}$, the transfer function demonstrates an oscillatory behavior and its amplitude grows faster. At very large momenta, $k/a_0 \gtrsim 10^{24}$ Mpc^{-1}, enhancement is absent and we observe the original spectrum. The picture is qualitatively similar to Fig. 1(d) in Ref. [55]. As it was mentioned above, we are interested in modes with momenta $k/a_0 \lesssim 1$ A.U. For these modes, we can consider the transfer function as a constant. Its dependence on α is shown in the right panel of Fig. 5.

There are some interesting features in the time evolution of the transfer function during preheating; see Fig. 6. For the modes with small momenta, which can survive diffusion, $k/a_0 < 1$ A.U.$^{-1}$, parametric resonance is rather inefficient and an amplification occurs only during the first oscillation of the inflaton (the blue line in Fig. 6). The situation changes for the modes with the physical momentum at the beginning of preheating $k_{ph} = k/a(\tau_0)$, which is comparable with the frequency of the inflaton oscillations μ. For these modes parametric resonance is more efficient and the amplitude grows during the first 5–10 oscillations; see the green line in Fig. 6. This causes the peak in the spectrum; see the left panel in Fig. 5. However, for larger momenta, the resonance does not occur at the beginning of the preheating stage and a stochastic behavior is observed (the red line in Fig. 6 for $\mu\tau < 60$). When the Universe's expansion redshifts the physical momentum to the values comparable with μ, the resonance turns on and we observe the amplification of the amplitude during a few oscillations (the red line in Fig. 6 for $60 < \mu\tau < 150$). This amplification is not as large as for the green line, because at the moment, when it starts, the value of the parameter q_M is smaller due to the Universe's expansion. This explains the decreasing "tail" of the spectrum in Fig. 5. Although these modes demonstrate a rather interesting behavior, they would not survive the diffusion during further evolution of the Universe, therefore, they do not contribute to the present value of the magnetic field.

Taking into account all previous results, we can now calculate the generated magnetic field:

$$B_0 = \sqrt{2\rho_B} = \sqrt{2\int_0^{k_{\rm diff}} \frac{dk}{k}\frac{d\rho_B}{d\ln k}}. \tag{32}$$

The strength of this magnetic field strongly depends on α. The corresponding dependence is plotted in Fig. 7. This figure implies that the magnetic fields which correspond to the present observations could be obtained for $\alpha \sim 12$–15.

IV. CONCLUSION

In this work, we studied the generation of large-scale magnetic fields in the Starobinsky model of inflation, which is favored by the latest results of Planck 2015 [48]. In order to break the conformal invariance of the electromagnetic action, we chose the kinetic coupling $f^2(\phi)FF$ of the inflaton field with the electromagnetic field through the exponential coupling function $f(\phi) = \exp(\alpha\phi)$, which does not cause the strong coupling problem during inflation. To the best of our knowledge, this form of coupling function in combination with the Starobinsky model of inflation has not been considered in the literature before.

In addition, we examined the possibility of further amplification of generated magnetic field during the preheating stage, when the inflaton oscillates in the vicinity of the minimum of its potential. During this stage, the Universe is effectively matter dominated, and the inflaton's amplitude of oscillations decreases in time. This reduces the effectiveness of the parametric resonance and causes the exponential amplification of magnetic field only during the first few oscillations of the inflaton field.

We found that it is possible in such a model to generate the large-scale magnetic fields with strength $\gtrsim 10^{-15}$ Gauss at the present epoch during the inflation and preheating stages in a certain range of the parameter $\alpha \sim 12$–15. The spectrum of generated magnetic fields is blue with the spectral index $n = 1 + s$, $s > 0$. When a certain mode crosses the horizon, its amplitude diminishes due to the Universe's expansion. Therefore, the earlier the mode crosses the horizon, the smaller the amplitude it has in the end. This explains the blue spectrum of generated magnetic fields. It is necessary to emphasize that near the end of inflation the evolution of the inflaton field starts to deviate from the slow-rolling regime and leads to a significant increase by modulus of the time derivative of the inflaton field. As we showed in Sec. III A, this causes an instability in the equation governing the evolution of the electromagnetic field. As a result, all modes which are outside the horizon at that time undergo amplification. This is a consequence of the three independent features of the model under consideration: (i) the effective potential of the Starobinsky model (2) causes the growth of $|\dot{\phi}|$ near the end of inflation, (ii) the exponential form of the kinetic coupling function produces the term $\alpha^2\dot{\phi}^2$ in Eq. (14), and (iii) large values $\alpha \gg 1$ lead to the domination of this term and to an instability. Of course, the modes that do not exit the horizon until the end of inflation undergo neither diminishment nor amplification and so remain unchanged.

According to Refs. [38,40,64], the kinetic coupling model often faces the backreaction problem. In the model considered in this paper, the kinetic coupling function does not scale like $f \propto a^\alpha$ during the inflation stage and, therefore, the backreaction could not be treated by the methods considered in Ref. [38]. Therefore, we used a numerical analysis and found that for a certain range of values of the coupling parameter, $\alpha = 12$–15, the model under consideration avoids the backreaction problem for all relevant modes. Other constraints on inflationary magnetogenesis are often enforced by the requirement that the backreaction of generated magnetic fields on the evolution of primordial curvature perturbations is small [40]. We plan to address this issue elsewhere.

We found also that the value of the generated magnetic field scales with the maximal temperature during preheating as $B_0 \propto T_{\max}^{s/2}$. Therefore, a lower maximal temperature $T_{\max}$ would give a lower value of B_0 for a given α. On the other hand, the energy density of electromagnetic fields at the end of inflation, which can cause the backreaction, scales like $\propto T_{\max}^{2+s}$ and decreases much faster compared to B_0 as $T_{\max}$ decreases. Therefore, lower values of $T_{\max}$ make it possible to extend the range of possible values of α.

Finally, we would like to mention that it would be interesting to extend our study by taking into account the role of chiral anomaly [68] and helicity [69] on the evolution of magnetic fields in the early Universe. According to Ref. [70], the inclusion of anomalous currents leads to an inverse cascade, where a part of the energy of magnetic fields is transferred from shorter to longer wavelengths and, thus, escapes the dissipation during the evolution of the Universe (for a recent discussion, see Ref. [71]). The role of inhomogeneities in primordial chiral plasma was addressed in Refs. [72,73]. By numerically studying the anomalous Maxwell equations, it was shown [74] that due to the effects of diffusion these inhomogeneities do not prevent the anomaly-driven inverse cascade. On the other hand, it was shown a long time ago [75] that the inverse cascade is driven by helical magnetic turbulence. Therefore, it is interesting and urgent to study the magnetohydrodynamics of the primordial plasma accounting for the effects of both chirality and turbulence. A first step in such an analysis was recently taken in Ref. [76].

ACKNOWLEDGMENTS

The work of S. V., E. V. G., and I. R. is supported partially by the Swiss National Science Foundation, Grant No. SCOPE IZ7370-152581. S. V. is grateful to the Swiss National Science Foundation (individual Grant No. IZKOZ2-154984). The authors are grateful to Professor Yuri Shtanov for useful comments and discussion. S. V. is grateful to Professor Marc Vanderhaeghen and Dr. Vladimir Pascalutsa for their support and kind hospitality at the Institut für Kernphysik, Johannes Gutenberg-Universität Mainz, Germany, where part of this work was done. O. S. is grateful to Professor Alexei Boyarsky and Professor Vadim Cheianov for their kind hospitality at the Instituut Lorentz, Universiteit Leiden, The Netherlands, where the final part of this work was done.

[1] M. Giovannini, The Magnetized universe, Int. J. Mod. Phys. D **13**, 391 (2004).
[2] P. P. Kronberg, Extragalactic magnetic fields, Rep. Prog. Phys. **57**, 325 (1994).
[3] L. M. Widrow, Origin of galactic and extragalactic magnetic fields, Rev. Mod. Phys. **74**, 775 (2002).
[4] A. Kandus, K. E. Kunze, and C. G. Tsagas, Primordial magnetogenesis, Phys. Rep. **505**, 1 (2011).

[5] D. Grasso and H. R. Rubinstein, Magnetic fields in the early universe, Phys. Rep. **348**, 163 (2001).
[6] R. Durrer and A. Neronov, Cosmological magnetic fields: their generation, evolution and observation, Astron. Astrophys. Rev. **21**, 62 (2013).
[7] K. Subramanian, The origin, evolution and signatures of primordial magnetic fields, Rep. Prog. Phys. **79**, 076901 (2016).
[8] P. A. R. Ade *et al.* (Planck Collaboration), Planck 2015 results. XIX. Constraints on primordial magnetic fields, Astron. Astrophys. **594**, A19 (2016).
[9] D. R. Sutton, C. Feng, and C. L. Reichardt, Current and Future Constraints on Primordial Magnetic Fields, arXiv:1702.01871.
[10] A. Neronov and I. Vovk, Evidence for strong extragalactic magnetic fields from Fermi observations of TeV blazars, Science **328**, 73 (2010).
[11] A. M. Taylor, I. Vovk, and A. Neronov, Extragalactic magnetic fields constraints from simultaneous GeV-TeV observations of blazars, Astron. Astrophys. **529**, A144 (2011).
[12] F. Tavecchio, G. Ghisellini, L. Foschini, G. Bonnoli, G. Ghirlanda, and P. Coppi, The intergalactic magnetic field constrained by Fermi/LAT observations of the TeV blazar 1ES $0229 + 200$, Mon. Not. R. Astron. Soc. **406**, L70 (2010).
[13] C. Caprini and S. Gabici, Gamma-ray observations of blazars and the intergalactic magnetic field spectrum, Phys. Rev. D **91**, 123514 (2015).
[14] C. J. Hogan, Magnetohydrodynamic Effects of a First-Order Cosmological Phase Transition, Phys. Rev. Lett. **51**, 1488 (1983).
[15] J. M. Quashnock, A. Loeb, and D. N. Spergel, Magnetic field generation during the cosmological QCD phase transition, Astrophys. J. **344**, L49 (1989).
[16] T. Vachaspati, Magnetic fields from cosmological phase transitions, Phys. Lett. B **265**, 258 (1991).
[17] B.-L. Cheng and A. V. Olinto, Primordial magnetic fields generated in the quark - hadron transition, Phys. Rev. D **50**, 2421 (1994).
[18] G. Sigl, A. V. Olinto, and K. Jedamzik, Primordial magnetic fields from cosmological first order phase transitions, Phys. Rev. D **55**, 4582 (1997).
[19] J. Ahonen and K. Enqvist, Magnetic field generation in first order phase transition bubble collisions, Phys. Rev. D **57**, 664 (1998).
[20] M. S. Turner and L. M. Widrow, Inflation produced, large scale magnetic fields, Phys. Rev. D **37**, 2743 (1988).
[21] V. F. Mukhanov and G. V. Chibisov, Quantum fluctuations and a nonsingular universe, JETP Lett. **33**, 532 (1981).
[22] S. W. Hawking, The development of irregularities in a single bubble inflationary universe, Phys. Lett. **115B**, 295 (1982).
[23] A. A. Starobinsky, Dynamics of phase transition in the new inflationary universe scenario and generation of perturbations, Phys. Lett. **117B**, 175 (1982).
[24] A. H. Guth and S. Y. Pi, Fluctuations in the New Inflationary Universe, Phys. Rev. Lett. **49**, 1110 (1982).
[25] J. M. Bardeen, P. J. Steinhardt, and M. S. Turner, Spontaneous creation of almost scale - free density perturbations in an inflationary universe, Phys. Rev. D **28**, 679 (1983).
[26] L. P. Grishchuk, Amplification of gravitational waves in an istropic universe, Sov. Phys. JETP **40**, 409 (1975).
[27] A. A. Starobinsky, Spectrum of relict gravitational radiation and the early state of the universe, JETP Lett. **30**, 682 (1979).
[28] V. A. Rubakov, M. V. Sazhin, and A. V. Veryaskin, Graviton creation in the inflationary universe and the grand unification scale, Phys. Lett. **115B**, 189 (1982).
[29] L. Parker, Particle Creation in Expanding Universes, Phys. Rev. Lett. **21**, 562 (1968).
[30] B. Ratra, Cosmological 'seed' magnetic field from inflation, Astrophys. J. **391**, L1 (1992).
[31] A. D. Dolgov, Breaking of conformal invariance and electromagnetic field generation in the universe, Phys. Rev. D **48**, 2499 (1993).
[32] M. Gasperini, M. Giovannini, and G. Veneziano, Primordial Magnetic Fields from String Cosmology, Phys. Rev. Lett. **75**, 3796 (1995).
[33] M. Giovannini, Magnetogenesis and the dynamics of internal dimensions, Phys. Rev. D **62**, 123505 (2000).
[34] K. Atmjeet, I. Pahwa, T. R. Seshadri, and K. Subramanian, Cosmological magnetogenesis from extra-dimensional gauss bonnet gravity, Phys. Rev. D **89**, 063002 (2014).
[35] M. Giovannini, On the variation of the gauge couplings during inflation, Phys. Rev. D **64**, 061301 (2001).
[36] K. Bamba and J. Yokoyama, Large scale magnetic fields from inflation in dilaton electromagnetism, Phys. Rev. D **69**, 043507 (2004).
[37] J. Martin and J. Yokoyama, Generation of large-scale magnetic fields in single-field inflation, J. Cosmol. Astropart. Phys. 01 (2008) 025.
[38] V. Demozzi, V. Mukhanov, and H. Rubinstein, Magnetic fields from inflation?, J. Cosmol. Astropart. Phys. 08 (2009) 025.
[39] S. Kanno, J. Soda, and M. Watanabe, Cosmological magnetic fields from inflation and backreaction, J. Cosmol. Astropart. Phys. 12 (2009) 009.
[40] R. J. Z. Ferreira, R. K. Jain, and M. S. Sloth, Inflationary magnetogenesis without the strong coupling problem, J. Cosmol. Astropart. Phys. 10 (2013) 004; Inflationary magnetogenesis without the strong coupling problem II: Constraints from CMB anisotropies and B-modes, J. Cosmol. Astropart. Phys. 06 (2014) 053.
[41] W. D. Garretson, G. B. Field, and S. M. Carroll, Primordial magnetic fields from pseudoGoldstone bosons, Phys. Rev. D **46**, 5346 (1992).
[42] M. M. Anber and L. Sorbo, N-flationary magnetic fields, J. Cosmol. Astropart. Phys. 10 (2006) 018.
[43] R. Durrer, L. Hollenstein, and R. K. Jain, Can slow roll inflation induce relevant helical magnetic fields?, J. Cosmol. Astropart. Phys. 03 (2011) 037.
[44] C. Caprini and L. Sorbo, Adding helicity to inflationary magnetogenesis, J. Cosmol. Astropart. Phys. 10 (2014) 056.
[45] T. Fujita, R. Namba, Y. Tada, N. Takeda, and H. Tashiro, Consistent generation of magnetic fields in axion inflation models, J. Cosmol. Astropart. Phys. 05 (2015) 054.

[46] M. M. Anber and E. Sabancilar, Hypermagnetic fields and baryon asymmetry from pseudoscalar inflation, Phys. Rev. D **92**, 101501(R) (2015).

[47] P. Adshead, J. T. Giblin, Jr., T. R. Scully, and E. I. Sfakianakis, Magnetogenesis from axion inflation, J. Cosmol. Astropart. Phys. 10 (2016) 039.

[48] P. A. R. Ade *et al.* (Planck Collaboration), Planck 2015 results. XX. Constraints on inflation, Astron. Astrophys. **594**, A20 (2016).

[49] A. A. Starobinsky, A new type of isotropic cosmological models without singularity, Phys. Lett. **91B**, 99 (1980).

[50] J. Ellis, D. V. Nanopoulos, and K. A. Olive, No-Scale Supergravity Realization of the Starobinsky Model of Inflation, Phys. Rev. Lett. **111**, 111301 (2013).

[51] J. Ellis, D. V. Nanopoulos, and K. A. Olive, Starobinsky-like inflationary models as avatars of no-scale supergravity, J. Cosmol. Astropart. Phys. 10 (2013) 009.

[52] W. Buchmüller, V. Domcke, and K. Kamada, The starobinsky model from superconformal D-term inflation, Phys. Lett. B **726**, 467 (2013).

[53] F. Farakos, A. Kehagias, and A. Riotto, On the starobinsky model of inflation from supergravity, Nucl. Phys. **B876**, 187 (2013).

[54] S. Ferrara, R. Kallosh, and A. Van Proeyen, On the supersymmetric completion of $R + R^2$ gravity and cosmology, J. High Energy Phys. 11 (2013) 134.

[55] T. Kobayashi, Primordial magnetic fields from the post-inflationary universe, J. Cosmol. Astropart. Phys. 05 (2014) 040.

[56] L. Kofman, A. D. Linde, and A. A. Starobinsky, Towards the theory of reheating after inflation, Phys. Rev. D **56**, 3258 (1997).

[57] I. Rudenok, Y. Shtanov, and S. Vilchinskii, Post-inflationary preheating with weak coupling, Phys. Lett. B **733**, 193 (2014).

[58] E. A. Calzetta and A. Kandus, Selfconsistent estimates of magnetic fields from reheating, Phys. Rev. D **65**, 063004 (2002).

[59] A. Díaz-Gil, J. García-Bellido, M. García Pérez, and A. González-Arroyo, Magnetic Field Production During Preheating at the Electroweak Scale, Phys. Rev. Lett. **100**, 241301 (2008).

[60] K. Jedamzik, M. Lemoine, and J. Martin, Collapse of small-scale density perturbations during preheating in single field inflation, J. Cosmol. Astropart. Phys. 09 (2010) 034.

[61] R. Easther, R. Flauger, and J. B. Gilmore, Delayed reheating and the breakdown of coherent oscillations, J. Cosmol. Astropart. Phys. 04 (2011) 027.

[62] J. T. Deskins, J. T. Giblin, Jr., and R. R. Caldwell, Gauge field preheating at the end of inflation, Phys. Rev. D **88**, 063530 (2013).

[63] P. Adshead, J. T. Giblin, Jr., T. R. Scully, and E. I. Sfakianakis, Gauge-preheating and the end of axion inflation, J. Cosmol. Astropart. Phys. 12 (2015) 034.

[64] T. Fujita and R. Namba, Pre-reheating magnetogenesis in the kinetic coupling model, Phys. Rev. D **94**, 043523 (2016).

[65] T. Faulkner, M. Tegmark, E. F. Bunn, and Y. Mao, Constraining $f(R)$ gravity as a scalar tensor theory, Phys. Rev. D **76**, 063505 (2007).

[66] J. D. Barrow, R. Maartens, and C. G. Tsagas, Cosmology with inhomogeneous magnetic fields, Phys. Rep. **449**, 131 (2007).

[67] T. Fujita and S. Mukohyama, Universal upper limit on inflation energy scale from cosmic magnetic field, J. Cosmol. Astropart. Phys. 10 (2012) 034.

[68] M. Joyce and M. E. Shaposhnikov, Primordial Magnetic Fields, Right-Handed Electrons, and the Abelian Anomaly, Phys. Rev. Lett. **79**, 1193 (1997).

[69] J. Cornwall, Speculations on primordial magnetic helicity, Phys. Rev. D **56**, 6146 (1997).

[70] A. Boyarsky, J. Fröhlich, and O. Ruchayskiy, Self-Consistent Evolution of Magnetic Fields and Chiral Asymmetry in the Early Universe, Phys. Rev. Lett. **108**, 031301 (2012).

[71] M. Sydorenko, O. Tomalak, and Y. Shtanov, Magnetic Fields and Chiral Asymmetry in the Early Hot Universe, J. Cosmol. Astropart. Phys. 10 (2016) 018.

[72] A. Boyarsky, J. Frohlich, and O. Ruchayskiy, Magnetohydrodynamics of chiral relativistic fluids, Phys. Rev. D **92**, 043004 (2015).

[73] E. V. Gorbar, I. A. Shovkovy, S. Vilchinskii, I. Rudenok, A. Boyarsky, and O. Ruchayskiy, Anomalous Maxwell equations for inhomogeneous chiral plasma, Phys. Rev. D **93**, 105028 (2016).

[74] E. V. Gorbar, I. Rudenok, I. A. Shovkovy, and S. Vilchinskii, Anomaly-driven inverse cascade and inhomogeneities in a magnetized chiral plasma in the early Universe, Phys. Rev. D **94**, 103528 (2016).

[75] A. Pouquet, U. Frisch, and J. Leorat, Strong MHD helical turbulence and the nonlinear dynamo effect, J. Fluid Mech. **77**, 321 (1976).

[76] M. Dvornikov and A. Semikoz, Influence of the turbulent motion on the chiral magnetic effect in the early Universe, Phys. Rev. D **95**, 043538 (2017).